

SUPPLEMENTAL MATERIAL

SUPPLEMENTARY MATERIALS AND METHODS

ImageJ based analysis of confocal microscopic pictures

The following macros were used to quantify mCherry-Parkin dots (A), mitochondrial mass (B), and the length of mitochondrial tubes (C):

(A) Confocal pictures were recorded in ten Z-stacks and analyzed with z-project [run("Z Project...", "projection=[Average Intensity]"); run("Split Channels");]. The MTC02 and mCherry-Parkin channels were made binary [selectWindow("Parkin.lsm"); run("Subtract Background...", "rolling=300 stack"); run("Auto Threshold", "method=MaxEntropy white"); selectWindow("MTC02.lsm"); run("Auto Threshold", "method=RenyiEntropy white");]. The number of mCherry-Parkin dots localized in the regions with MTC02 signals were analyzed with the plugin "Speckle Inspector" [2] [run("Speckle Inspector", "big=MTC02.tif small=Parkin.tif min_object=3 min_object_circularity=0.3 min_speckle_size=3 max_speckle_size=50 exclude roi speckle");].

(B) Confocal pictures were recorded in ten and more Z-stacks and analyzed with z-project [run("Z Project...", "projection=[Average Intensity]"); run("Split Channels");]. Further on α -Tubulin signal was reduced to a binary picture [run("Median...", "radius=4"); run("Subtract Background...", "rolling=200"); run("Auto Threshold", "method=Li dark");]. MTC02 signal was detected in regions of interest of the α -Tubulin signal [run("Analyze Particles...", "size=50-Infinity add"); selectWindow(MTC02); roiManager("Measure");].

(C) Confocal pictures were recorded in ten and more Z-stacks and analyzed with z-project [run("Z Project...", "projection=[Average Intensity]"); run("Split Channels");]. The MTC02 channel was made binary [run("Subtract Background...", "rolling=300 stack"); run("Auto Threshold", "method=Default dark");]. The mitochondrial length was measured by "Particle Length (via Skeleton)" [2] [run("Analyze Particles...", "size=0,3-Infinity show=Outlines display");].

Measurement of BrdU incorporation

Primary human dermal fibroblasts were transfected with miR-15b-inhibitors with co-transfection of siRNA duplexes against SIRT4 or control siRNA duplexes.

Following two days, cells were incubated for another two days in culture media containing 10 μ M BrdU. Staining of fixed cells and further FACS analysis were performed as described in the BrdU staining kit (556029, BD Biosciences). DNA was stained for 10 min with 7-AAD (10 μ l/10⁶ cells; 00-6993-50, eBioscience™).

Quantification of mitochondrial mass by MitoTracker® FACS

HEK293 cells were stained with the cell-permeable dye MitoTracker® Deep Red FM (100 μ M; Thermo Fisher Scientific) for 20 min followed by flow cytometry using a BD FACSCanto™ II system (BD Biosciences) and Flowing Software 2.5.1 (University of Turku, Finland) or FlowJo V10 (FlowJo, LLC).

Immunoprecipitation of OPA1 from stably transfected HEK293 cells

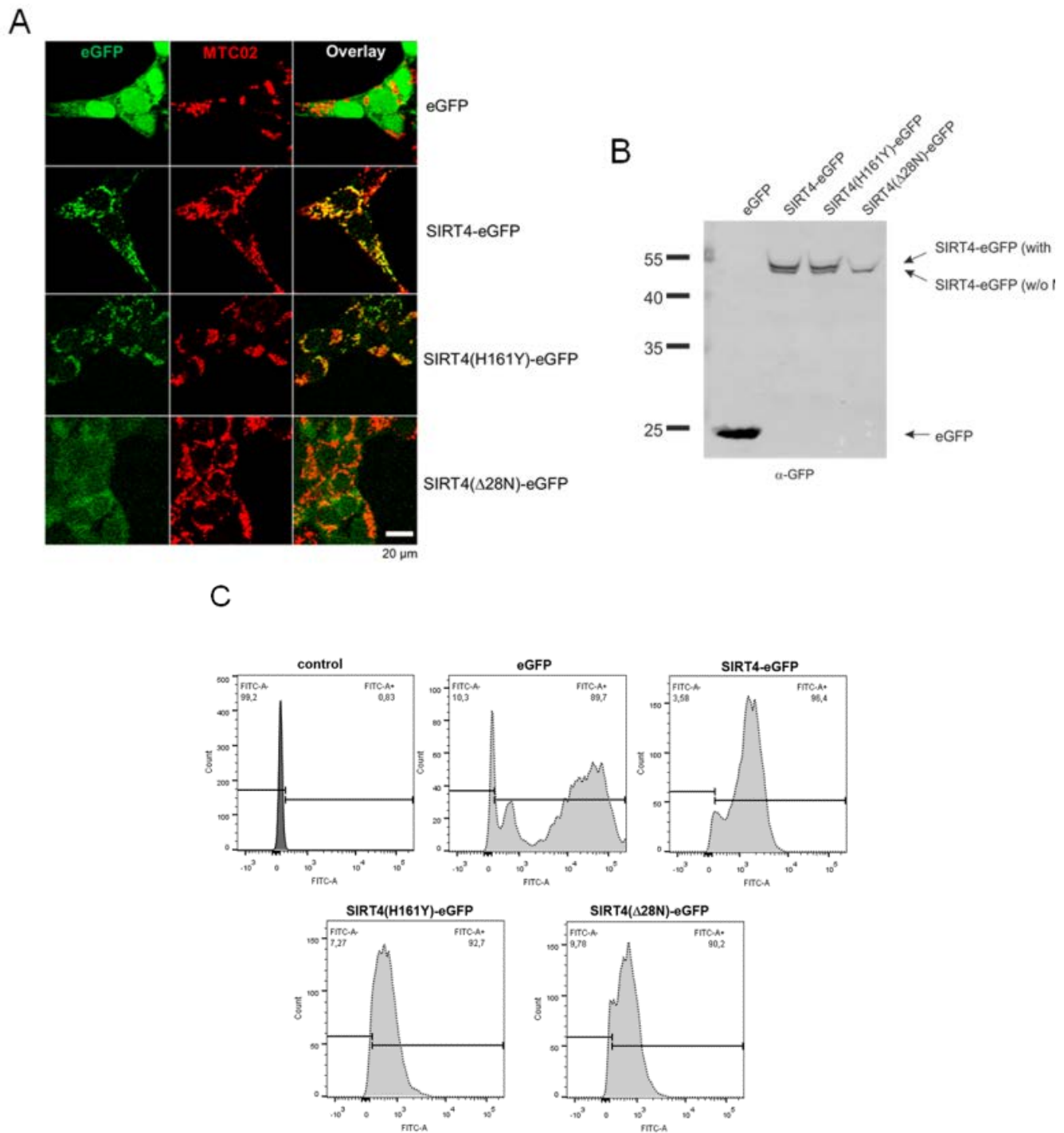
Total cell lysates from HEK293 cells stably expressing eGFP, SIRT4-eGFP, SIRT4(H161Y)-eGFP, or SIRT4(Δ 28N)-eGFP were prepared as described above. Two mg protein was incubated with 0.5 μ l rabbit anti-OPA1 antibody [3] in a total volume of 300 μ l lysis buffer [0.3% CHAPS, 50 mM Tris-HCl (pH 7.4), 150 mM NaCl, 1 mM Na₃VO₄, 10 mM NaF, 1 mM EDTA, 1 mM EGTA, 2.5 mM Na₄O₇P₂, 1 μ M DTT, 1x cOmplete™ protease inhibitor cocktail (Roche)] overnight at 4°C. Protein A/G sepharose beads (Santa Cruz Biotechnology 10 μ l beads in 100 μ l lysis buffer) were added and followed by incubation for two hours at 4°C under rotation. The beads were washed four-times with 1 ml washing buffer (lysis buffer without cOmplete™ protease inhibitor cocktail) followed by incubation in Laemmli loading buffer at 95°C for 5 min. Samples and total cell lysates (5% of input) were subjected to SDS-PAGE (10% gels) and proteins were transferred to nitrocellulose membranes (Hybond C, GE Healthcare). Membranes were incubated overnight at 4°C with antibodies against GFP (11814460001, Roche Molecular Systems) and OPA1 (612607, BD Biosciences) diluted 1:1000 in TBS containing 0.05% Tween 20.

SUPPLEMENTARY REFERENCES

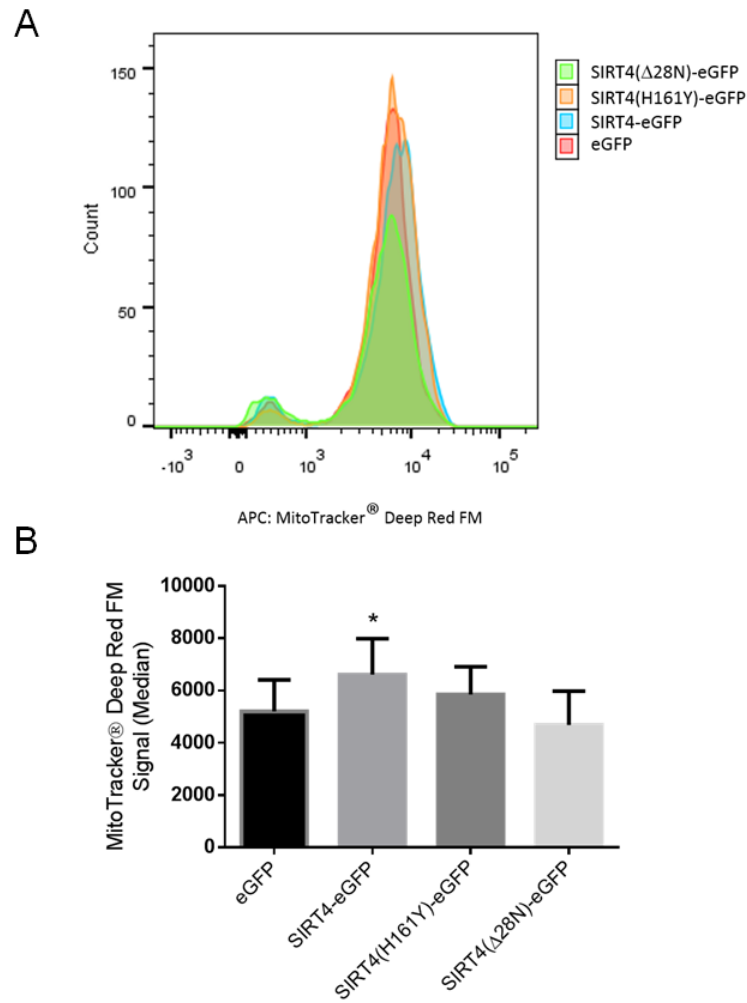
1. Lang A, Grether-Beck S, Singh M, Kuck F, Jakob S, Kefalas A, Altinoluik-Hambuchen S, Graffmann N, Schneider M, Lindecke A, Brenden H, Felsner I, Ezzahoini H, et al. MicroRNA-15b regulates mitochondrial ROS production and the senescence-associated secretory phenotype through sirtuin 4/SIRT4. *Aging* (Albany NY). 2016; 8:534-559. <https://doi.org/10.18632/aging.100905>

2. Brocher J. The BioVoxel Image Processing and Analysis Toolbox. EuBIAS-Conference. 2015, Jan 5.
3. Barrera M, Koob S, Dikov D, Vogel F and Reichert AS. OPA1 functionally interacts with MIC60 but is dispensable for crista junction formation. FEBS Lett. 2016; 590(19):3309-3322.
<https://doi.org/10.1002/1873-3468>

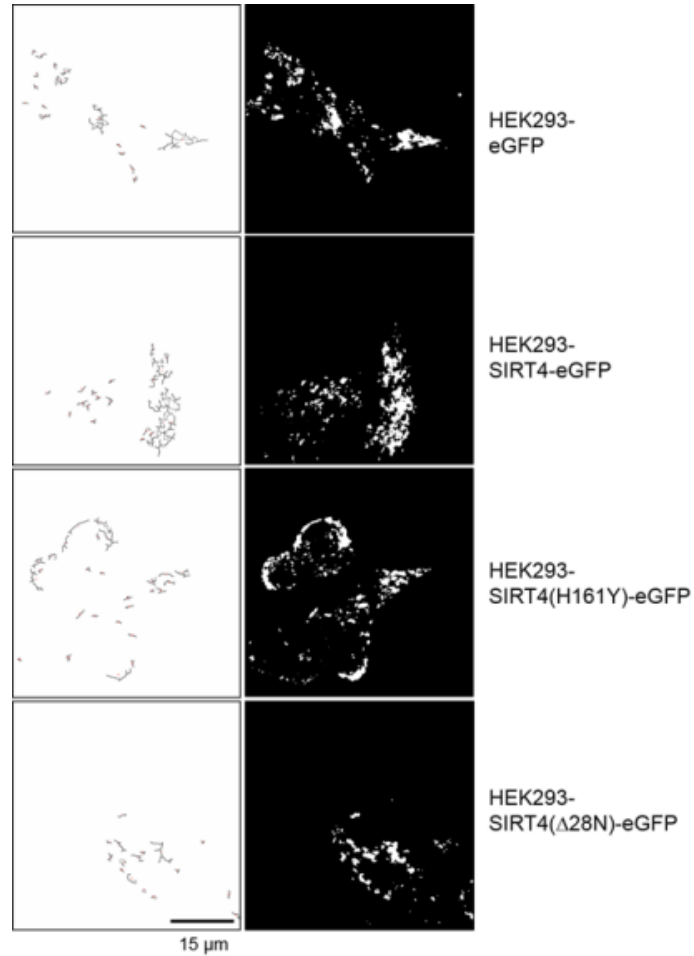
SUPPLEMENTARY FIGURES



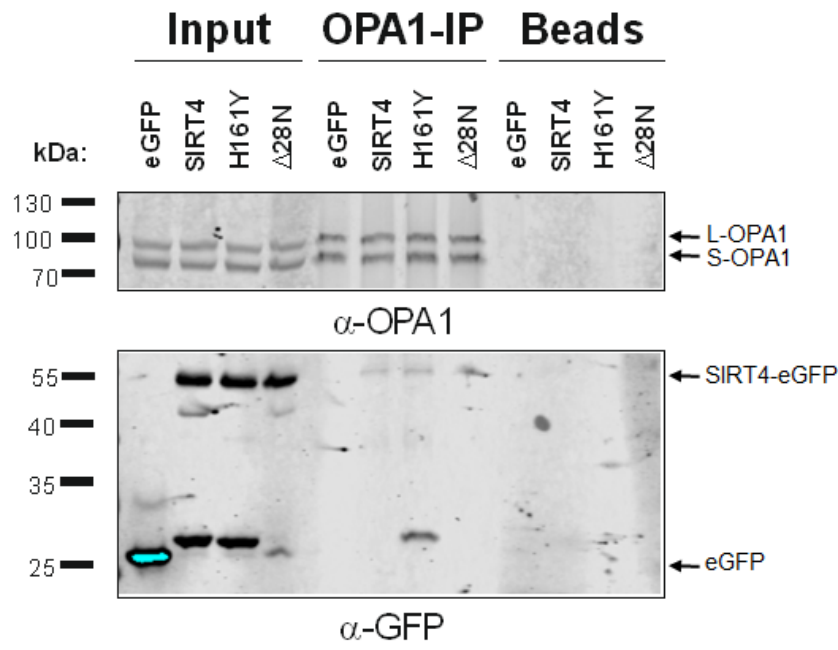
Supplementary Figure S1. Validation of subcellular localization and expression of eGFP, SIRT4-eGFP, SIRT4(H161Y)-eGFP, and SIRT4(Δ28N)-eGFP in HEK293 cells. HEK293 cells expressing eGFP, SIRT4-eGFP, SIRT4(H161Y)-eGFP, or SIRT4(Δ28N)-eGFP were subjected to confocal microscopic (A), immunoblot (B), and flow cytometric (C) analysis. MTS, mitochondrial translocation sequence. Representative experiments are depicted.



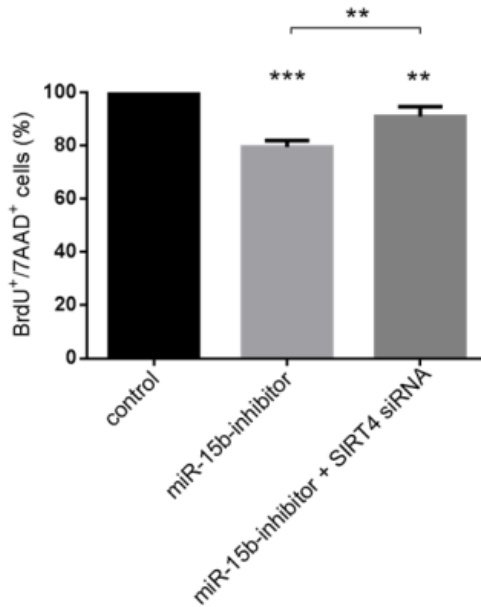
Supplementary Figure S2. SIRT4-eGFP expression results in a higher mitochondrial mass in HEK293 cells. (A) Representative flow cytometry profile of HEK293 cells expressing eGFP, SIRT4-eGFP, SIRT4(H161Y)-eGFP, or SIRT4(Δ28N)-eGFP stained with MitoTracker® Deep Red FM. (B) Quantitative analysis of MitoTracker® Deep Red FM signals. To evaluate statistical significance, two-way ANOVA followed-up Tukey's test was performed (* $p < 0.05$; $n = 3$ experiments).



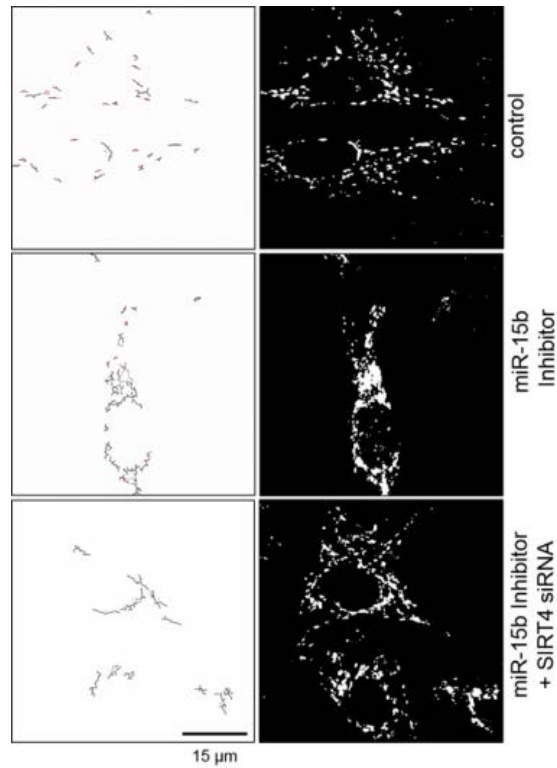
Supplementary Figure S3. Visualization and analysis of the length of fused mitochondria in HEK293 cells stably expressing SIRT4-eGFP or its mutants. Tracking of fused mitochondria which were detected by MTCO2 staining (right panels) was analyzed by an ImageJ software based Macro (left panels; Material and Methods & suppl. Material and Methods).



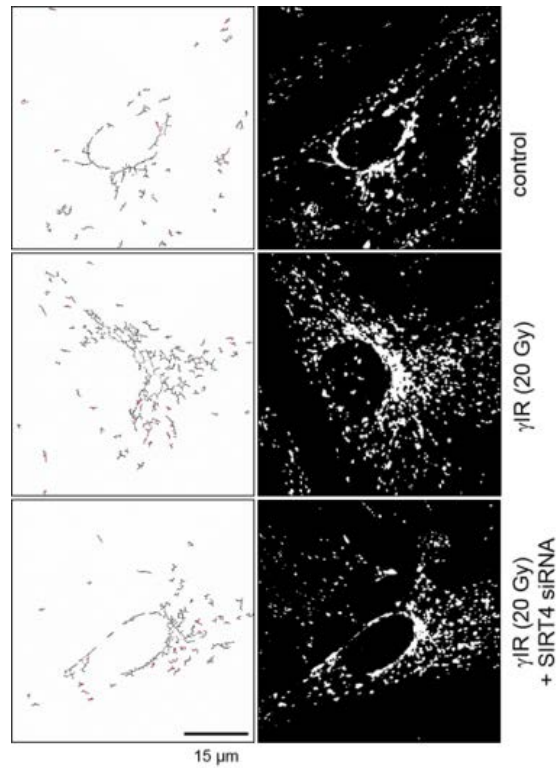
Supplementary Figure S4. Co-immunoprecipitation of OPA1 and SIRT4-eGFP. Total cell lysates from HEK293 cells stably expressing SIRT4-eGFP, SIRT4(H161Y)-eGFP, or SIRT4(Δ 28N)-eGFP were subjected to immunoprecipitation analysis (OPA1-IP) using a rabbit anti-OPA1 antibody (suppl. Material & Methods) followed by detection of co-immunoprecipitated SIRT4-eGFP. Total cell lysates were loaded as input control (5%) and samples w/o antibody employed as beads control.



Supplementary Figure S5. SIRT4 upregulation upon transfection of miR-15b inhibitors inhibits BrdU incorporation in primary human dermal fibroblasts. Primary human dermal fibroblasts were transfected with miR-15b inhibitors (or control oligonucleotides) in the presence or absence of siRNA duplexes against SIRT4 [35] and cultured for two days. Cells were thereafter pulsed with BrdU for another two days and thereafter subjected to FACS analysis. To evaluate statistical significance, two-way ANOVA followed by Tukey's test was performed (* p <0.05; n =3 experiments).



Supplementary Figure S6. Visualization and analysis of the length of fused mitochondria in primary human dermal fibroblasts upon SIRT4 upregulation through miR-15b inhibition. Tracking of fused mitochondria which were detected by MTCO2 staining (right panels) was analyzed by an ImageJ software based Macro (left panels; Material and Methods & suppl. Material and Methods).



Supplementary Figure S7. Visualization and analysis of the length of fused mitochondria in primary human dermal fibroblasts upon γ -irradiation. Tracking of fused mitochondria which were detected by MTCO2 staining (right panels) was analyzed by an ImageJ software based Macro (left panels; Material and Methods & suppl. Material and Methods).

SUPPLEMENTARY MOVIES

Please browse the Full text version of this manuscript to see the Supplementary Movies 1-10.

Suppl. Movie 1: 3D reconstruction of the mitochondrial network in HEK293-eGFP cells. Mitochondria were detected by MTC02 staining and spinning disk confocal microscopic analysis.

Suppl. Movie 2: 3D reconstruction of the mitochondrial network in HEK293-SIRT4-eGFP cells. Mitochondria were detected by MTC02 staining and spinning disk confocal microscopic analysis.

Suppl. Movie 3: 3D reconstruction of the mitochondrial network in HEK293-SIRT4(H161Y)-eGFP cells. Mitochondria were detected by MTC02 staining and spinning disk confocal microscopic analysis.

Suppl. Movie 4: 3D reconstruction of the mitochondrial network in HEK293-SIRT4(Δ 28N)-eGFP cells. Mitochondria were detected by MTC02 staining and spinning disk confocal microscopic analysis.

Suppl. Movie 5: 3D reconstruction of the mitochondrial network in primary human dermal fibroblasts. Mitochondria were detected by MTC02 staining and spinning disk confocal microscopic analysis.

Suppl. Movie 6: 3D reconstruction of the mitochondrial network in primary human dermal fibroblasts transfected with miR-15b inhibitors. Mitochondria were detected by MTC02 staining and spinning disk confocal microscopic analysis.

Suppl. Movie 7: 3D reconstruction of the mitochondrial network in primary human dermal fibroblasts transfected with miR-15b inhibitors and siRNA duplexes against SIRT4. Mitochondria were detected by MTC02 staining and spinning disk confocal microscopic analysis.

Suppl. Movie 8: 3D reconstruction of the mitochondrial network in primary human dermal fibroblasts (sham treated). Mitochondria were detected by MTC02 staining and spinning disk confocal microscopic analysis.

Suppl. Movie 9: 3D reconstruction of the mitochondrial network in primary human dermal fibroblasts subjected to γ -irradiation (20 Gy). Mitochondria were detected by MTC02 staining and spinning disk confocal microscopic analysis.

Suppl. Movie 10: 3D reconstruction of the mitochondrial network in primary human dermal fibroblasts subjected to transfection with siRNA duplexes against SIRT4 and γ -irradiation (20 Gy). Mitochondria were detected by MTC02 staining and spinning disk confocal microscopic analysis.